A three dimensional model for osteocyte-regulated remodling simulation at the tissue level

A THREE DIMENSIONAL MODEL FOR OSTEOCYTE-REGULATED REMODELING SIMULATION AT THE TISSUE LEVEL

B. van Rietbergen[1], M.G. Mullender[1] and R. Huiskes[2]

1. ABSTRACT

Several hypothetical bone remodeling models have been developed to explain trabecular bone adaptation as observed in the skeleton. So far, these simulation models have been successfully used to explain the global density distribution in whole bones but were unable to simulate trabecular adaptation process at the tissue level.
In the presents study, a three dimensional bone remodeling model is introduced to simulate bone remodeling at the tissue level. The model is based on an osteocyte regulated bone remodeling hypothesis. The trabecular architecture is represented by large FE-models build of identical elements to allow the application of fast solving methods.
It was found that the model can explain the generation of typical three-dimensional architectures during morphogenesis as a result of loading. In addition, the model can explain structural changes that take place due to bone disuse.

2. INTRODUCTION

It has generally been accepted that the trabecular architecture in bone is the result of a dynamic remodeling process in response to mechanical loading. However, how the processes involved in bone remodeling are regulated is not known. Biological observations have suggested that the remodeling process can be schematized by a local control process in which sensor cells in the bone matrix measure a mechanical signal and mediate actor cells to add or remove bone in their vicinity [1-4]. Based on

Keywords: Bone remodeling, Trabecular bone, Microstructural modeling

[1] PhD student, Biomechanics Section, Institute of Orthopaedics, University of Nijmegen, P.O.Box 9101, 6500 HB, Nijmegen, The Netherlands
[2] Professor, Biomechanics Section, Institute of Orthopaedics, University of Nijmegen, P.O. Box 9101, 6500 HB, Nijmegen, The Netherlands

these observations a number of hypothetical remodeling models have been developed to describe the process in mathematical form [5-7]. Using FE-models of whole bones to calculate the mechanical stimulus as a function of bone density, it has been shown that many of these models can explain the density distribution and adaptation in bones as a result of the loading of the bone [5,7-10].

Although these models have proved to be successful in predicting bone density, several shortcomings have been recognized. One of the major shortcomings of these models is the fact that they simulate the effect of the remodeling process in a homogenized piece of bone rather than the physiological trabecular process itself. Consequently, these models can not distinguish between different bone remodeling models with the same net bone remodeling effect. Another important shortcoming of these models is that the mechanical behavior of bone is described by its density only, thus not accounting for the trabecular architecture.

Recently, models have been developed to overcome these shortcomings by simulating the bone remodeling process at the level where it actually takes place, i.e. the tissue level [11-14]. In these models the bone tissue is represented by finite element models, thus taking into account the trabecular architecture and allowing a physiological interpretation of parameters involved in the remodeling process. The large number of elements that is needed to model even a small region of bone in such detail inhibits, as yet, the application of these remodeling analyses to whole bones. It has been shown, however, that these simulation models can produce realistic trabecular architectures in small pieces of bone. The validation of these results, however, is hampered by the fact that only two-dimensional models have been used, whereas the trabecular architecture is essentially a three-dimensional one. So far, the large computational needs for the iterative solution of FE-models has inhibited the application of three-dimensional models for the simulation of bone remodeling at the tissue level, even for the small volumes considered. However, with increasing computer capacity and the recent development of fast solving techniques for large scale FE-models [15,16], it is now possible to drastically reduce the computer time required, thus bringing three-dimensional analyses within reach.

The purpose of the present study was to develop such a three dimensional model that makes use of these newly developed solving techniques and to simulate a hypothetical osteocytes regulated bone modeling and remodeling process. For this, first it is studied if the model can explain the typical bone architecture found throughout the body as a result of bone formation under specific loading conditions. Second, it is studied if the model can explain bone resorption patterns due to bone disuse.

3. METHODS

3.1 Mathematical formulation of the osteocyte regulated remodeling hypothesis

The remodeling hypothesis [13,14,17] assumes that osteocytes, forming a network in the mineralized bone tissue measure a mechanical signal S, which is assumed to be the strain energy density (dimensions: J/mm^3). It is further assumed that the osteocytes stimulate Basic Multicellular Units (BMU's) of osteoclasts and osteoblasts

[1,4,18,19] to model or remodel bone, dependent on the difference between the signal measured by the osteocyte (S) and a reference value k. The influence of this stimulus is assumed to decrease exponentially with the distance from the osteocyte, according to a spatial influence function:

$$f_i(\underline{x}) = e^{d_i(\underline{x})/D}, \tag{1}$$

where f_i is the influence of osteocyte i on the BMU at location $\underline{x}$, $d_i(\underline{x})$ is the distance between osteocyte i and location $\underline{x}$, and D (mm) represents the distance from an osteocyte at which location its effect has reduced to e^{-1}, i.e. 36.8 percent.
The local stimulus received by a BMU at location $\underline{x}$ at time t is the sum of the stimuli received from all osteocytes:

$$F(\underline{x},t) = \sum_{i=1}^{N_{ost}} f_i(\underline{x})(S_i - k) , \tag{2}$$

with N_{ost} the number of osteocytes. The relative mineralization $m(\underline{x},t)$ is regulated by the stimulus $F(\underline{x},t)$ according to:

$$\frac{dm(\underline{x},t)}{dt} = \tau F(\underline{x},t), \qquad with\ 0<m(\underline{x},t)\leq 1 , \tag{3}$$

where τ ($MPa^{-1}\ s^{-1}$) is a time constant regulating the rate of the process. The elastic properties of the bone tissue $E(\underline{x},t)$ were calculated from its relative mineralization $m(\underline{x},t)$, using a cubic power law [13,14]:

$$E(\underline{x},t) = Cm(\underline{x},t)^{\gamma} , \tag{4}$$

where C (MPa) and γ are constants.

3.2 Numerical formulation and considerations

Simulation of the bone remodeling process involves solving the initial value problem described by eq. (3). Due to the complexity of the calculation of the local stimulus $F(\underline{x},t)$, explicit solving of this problem is not possible. Instead, a numerical integration technique (forward Euler) is used. For this eq. (3) is rewritten to:

$$\frac{\Delta m(\underline{x},t)}{\Delta t} = \tau F(\underline{x},t) , \tag{5}$$

where Δm represents the change in bone mass during a small but finite time step Δt. Equation (5) is then solved recursively at incremental time intervals. At each increment the local stimulus $F(\underline{x},t)$ must be determined, requiring the calculation of the mechanical signal S_i at the osteocyte locations. For this, the domain is represented by a finite element model in which each element represents an equal volume of bone tissue with material properties calculated from the relative mineralization (eq. 4). Solving the FE-problem gives the mechanical signal at each location in the bone as a function of bone architecture and relative mineralization. By making assumptions about the distribution of the osteocytes throughout the domain, the location of each

osteocyte is known, and the stimulus can be calculated.

The choice of the time step Δt determines the accuracy and the stability of the numerical solution. Choosing a small time step requires frequent evaluation of eq. (2), which is computational expensive, as each evaluation requires the solving of the FE-problem. On the other hand, a large time step can give inaccurate and oscillating results [20,21] (Fig. 1). To avoid such problems, a time step is calculated in each increment, based on the maximal stimulus at any location F_{max} and a prescribed maximal allowable change in density $(\Delta m)_{max}$:

$$\Delta t = \frac{(\Delta m)_{max}}{\tau F_{max}} \tag{6}$$

With this approach, a density change of $(\Delta m)_{max}$ is enforced at one particular location in the model at every increment, resulting in small time steps at the start (i.e. just after a load change), and larger time steps later.

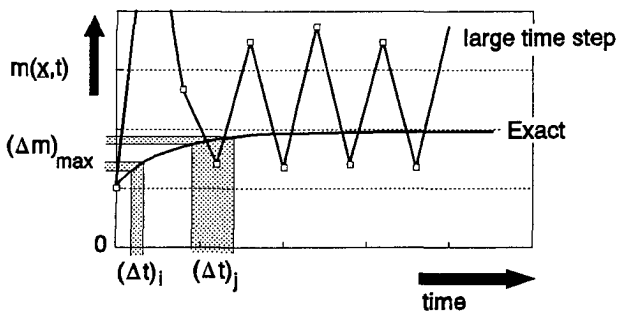

Fig.1 Choosing a small time step for the numerical integration is computational expensive, a large time step however can result in inaccuracies. These problems can be avoided by choosing a variable time step based on the resulting density changes.

3.3 Implementation of identical-element FE-models to solve large-scale three-dimensional FE-problems

For the FE-formulation the domain is subdivided in equally sized subdomains which, in analogy with 3-D reconstruction terminology, will be called voxels. The material properties in each voxel are described by its average relative mineralization $m(\underline{x},t)$ and are assumed homogenous in each voxel. Material properties are assigned only to the voxels that represent the bone tissue material; voxels representing the interstitial space are assigned a zero value. Note that $m(\underline{x},t)$ thus represents both the architecture and the material properties of the bone tissue. The number of voxels determines the resolution of the model. Due to the three-dimensionality and the small scale of the details, a large number of voxels is required (order 10^5), to model a volume of bone of the same size and refinement as used in earlier two-dimensional studies. A FE-model is then created by converting the voxels that represent bone tissue to elements in a FE-model, using a special preprocessor routine. The preprocessing consists of three stages. First it is checked if the bone voxels are connected to the main structure via at least one face-to-face connection with a neighboring element. Only those voxels are converted to elements, the others are removed to avoid singularities and

numerical inaccuracies during the solving of the FE-problem. Second, node numbers are assigned to the corners of the bone voxels and the element connectivities are calculated. Third, boundary conditions are applied at element faces that represent the boundaries of the domain.

The large number of elements in the resulting FE-model (order 10^4-10^5) inhibits the application of standard FE-codes for solving, due to computer time and space limitations. Instead, a special-purpose solving algorithm is used that can exploit the fact that all elements in the FE-model have the same size, geometry and orientation. This algorithm uses an iterative solver (Preconditioned Conjugate Gradient), in combination with an Element-By-Element matrix vector multiplication scheme [15,16,22]. For the FE-problems considered, this matrix-vector method is very efficient. As the Young's modulus is the only variable describing the material properties, only one element stiffness matrix has to be stored with a unit Young's modulus. The stiffness matrix for each element can then be calculated by multiplying this unit-stiffness matrix with the actual Young's modulus.

After solving the FE-problem, the strain energy density is calculated for each element from the element nodal displacements and forces. For those elements that are assumed to hold an osteocyte (not necessarily all elements), the calculated element strain energy density represents the mechanical signal S_i, from which the stimulus in the environment is calculated according to eq. (2).

3.4 Implementation of the osteocyte regulated remodeling algorithm

To calculate the relative mineralization for the next time step, the local stimulus $F(\underline{x},t)$, must be calculated for each voxel. For this purpose, the stimuli generated by the osteocytes must be weighted by the spatial influence function (eq. 1). With N_{vox} voxels and N_{ost} osteocytes in the model, this requires the evaluation of eq. (1) N_{vox}xN_{ost} times, with N_{vox} and N_{ost} on the order of 10^4-10^5. As each evaluation involves the calculation of distance d (i.e. calculating a square root), and the calculation of the exponential function, the stimulus calculation is computationally expensive. To reduce the calculation time, all possible values of the spatial influence function are calculated beforehand at discrete intervals, corresponding to the element centers. The calculated values are stored as 'weight-factors' in a three-dimensional array. The number of calculations is further reduced by calculating only the contributions of osteocytes in the neighborhood of a voxel. The dimension of this region is determined by the distance at which the weight-factors has dropped below 0.1 at any location in that voxel (Fig. 2).

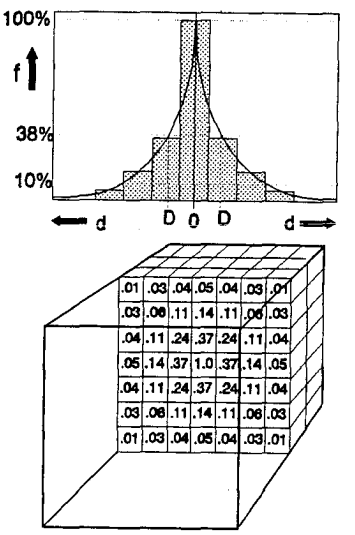

Fig. 2. Values for the spatial influence function (eq. 1) were calculated at discreet intervals corresponding with the element centers. The values are stored in a 3-D array as schematically indicated in the figure.

After calculating the stimulus, the new relative mineralization (eq. 5) is calculated and stored for each voxel. The sequence of calculations involved in the remodeling simulation is summarized in Fig. 3.

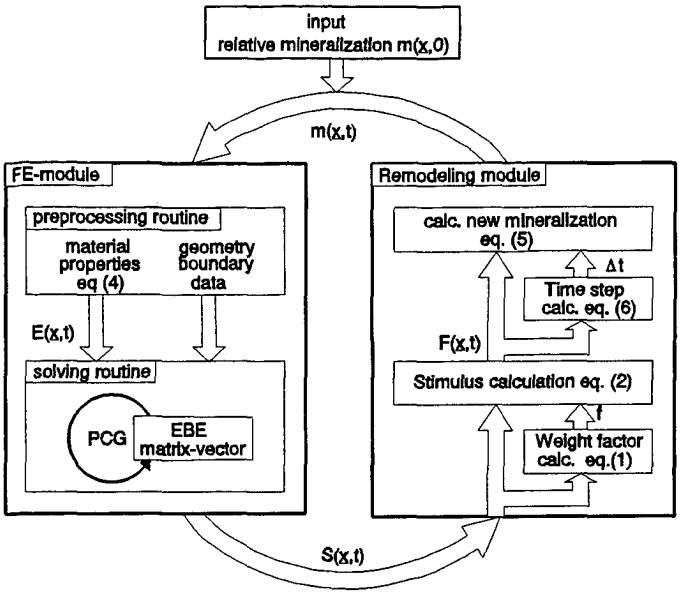

Fig. 3 Schematic overview of the remodeling simulation model.

3.5 Sample problems for the simulation of bone morphogenesis

A FE-model of a 1x1x1 mm piece of bone was modeled, using 40 voxels at each side of the cube, hence a maximum of 64,000 elements. In the initial configuration (Fig. 4) the FE-model forms a lattice framework constructed from partially mineralized bars (relative mineralization of 0.3). This initial configuration represents primary spongiosa formed prior to trabecular bone [18]. Parameters in the model were chosen in a physiological range: the osteocyte density was taken as 64,000 mm^{-3} [23] corresponding to one osteocyte at the center of each voxel. The reference stimulus of the osteocytes k (eq. 2) was calculated from the physiological strain [24] and the maximum Young's modulus and was taken as 0.02 J. The value for the osteocyte influence parameter D (eq. 1) was based on two-dimensional studies [13,14] and was taken equivalent to two element widths, i.e. 0.05 mm. Consequently, the influence of the osteocytes is limited to 6 element widths, beyond that limit their influence has dropped below 10 percent and is neglected.

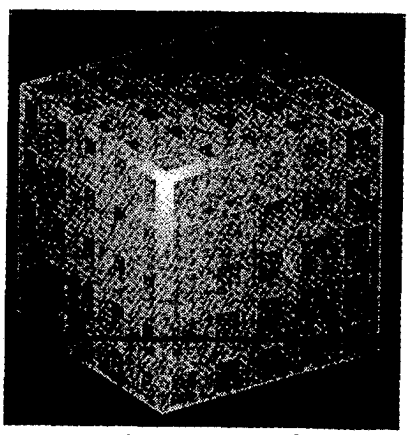

Fig. 4 In the initial configuration the FE-model represents a lattice structure.

The maximal Young's modulus of the tissue material was taken as 5000 MPa [25,26], this implies that the constant C in eq. (4) was set to 5000 MPa. The power in this equation was taken

as γ=3 [27]. The time constant τ was arbitrary set at τ= 1 $MPa^{-1}s^{-1}$, this means that the rate of the remodeling is represented in arbitrary simulation-time-units.
The loading of the FE-model was varied to represent three different cases. In the first case the stress distribution on the model was chosen to represent the local stress situation for a bone loaded in bending. For this a distributed ramp load was applied at the top and bottom face, whereby the load was varied linearly from 2 to 8 MPa (Fig. 5a). In the second case the loading of the model represents the local stress situation for a bone loaded in compression. In this case, a distributed normal compressive stress of 8 MPa in uniaxial compression was applied to the top and bottom face (Fig. 5b). In both cases constraints were applied to the side-faces such that no displacements were allowed perpendicular to these faces. The third case represents a combination of a distributed shear loading with a distributed compression loading, applied at the top, bottom and two side faces (Fig. 5c); the resultant stress magnitude at each face was 2 MPa. For all cases a minimum of additional constraints was applied to prevent rigid-body motions.
All simulations were run for 50 increments after which stable configurations were reached.
The configuration thus obtained were used as the initial configurations for the second part of the analyses where bone resorption due to disuse was studied. For this, the load on the resulting configurations was reduced by 40% and the simulation were continued for another 50 increments.
The geometry of the resulting architecture is visualized by showing only the elements that are mineralized beyond a threshold value of 0.1.

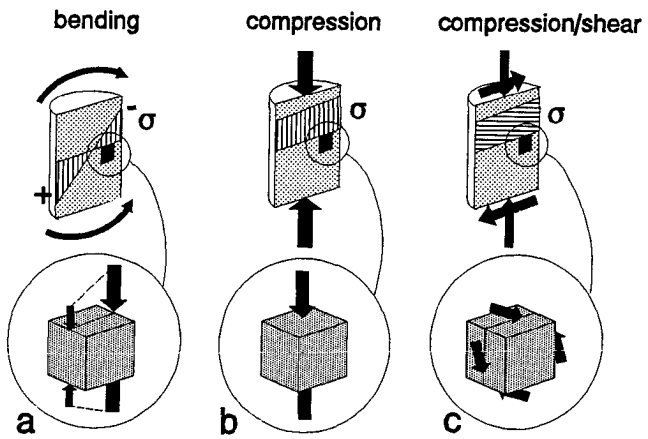

Fig. 5 The three loading cases. σ represents the local stress which is applied to the FE-model.

4. RESULTS

The average incremental computer time needed for the simulations varied between approximately 75 and 160 seconds using one processor of a Cray C98 computer. The preprocessing routine accounts for 0.9 percent, the solving routine for 81 percent and the remodeling routine for 17 percent of the computertime.

For the model with a distributed ramp load, the initial lattice structure is transformed to a strut-like structure (Fig. 6a), with struts oriented in the overall load direction. No transversal struts were found. The trabecular thickness is increased towards the

increasing load direction, ranging from 125 to 325 microns. For the model loaded with an axial compressive force, a closed void structure is generated (Fig. 6b), with an average width of 360 microns. For the model with the combined compressive/-shear loading a plate-like architecture is found with an average plate thickness of 100 microns (Fig. 6c).
In all cases the trabecular width is increased towards the loaded faces, forming thin end plates of dense bone at the these faces.

Starting with the configurations shown in Fig. 6, the results for the second series of simulation, whit the loading reduced by 40%, are shown in Fig. 7. For the model with a distributed ramp loading, the overall structure was similar, but the trabecular thickness was reduced, now ranging from 100 to 300 micron. For the model with an uniaxial compressive force, the closed void structure was transformed to an open columnar structure. The average trabecular width was reduced to 310 micron. For the model with a combined compressive/shear loading, holes were formed in the initial plate-like structure. In the resulting trabecular structure, the trabeculae are oriented in the overall load direction.

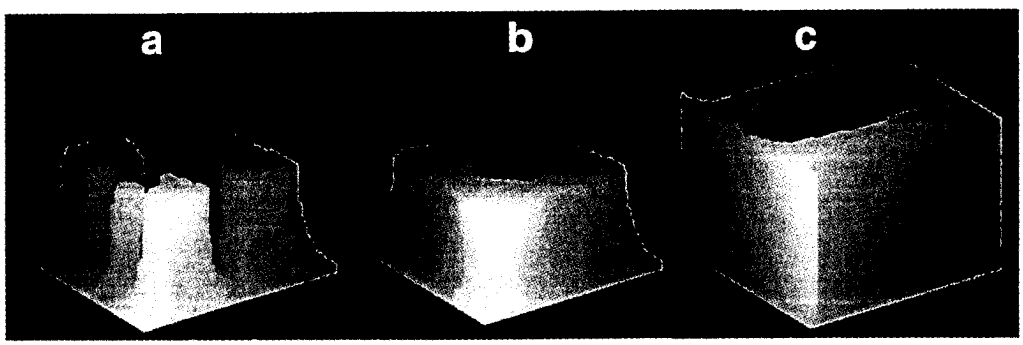

Fig. 6 The trabecular structures generated for the three loading cases, starting with the lattice structure shown in Fig.4. To reveal the inner structure, only the lower half of the models is shown.

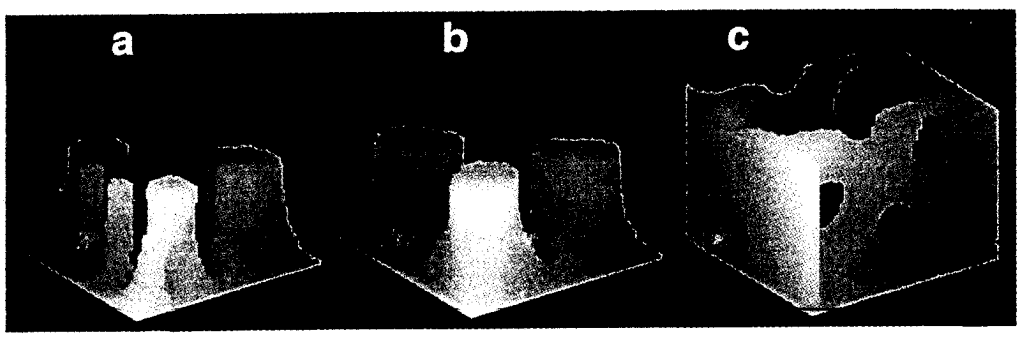

Fig. 7 Generated structures after the loading was reduced by 40%, starting with the configurations shown in Fig.6.

5. DISCUSSION

With the newly developed model, it is now possible to simulate three-dimensional bone remodeling and bone morphogenetic processes at the tissue level. Due to the three-dimensionality of the model, the results of the simulations can be characterized by the same structural parameters as used for real bone structures, thus offering opportunities for a rigorous validation of hypothetical models. Another advantage is the fact that the model can explain the generation of some typical three-dimensional structures, such as plate-like architectures, that can not be found in two-dimensional analyses.

Using this model it was shown that the osteocyte regulated bone adaptation model can explain the generation of typical three-dimensional trabecular architectures as a result of loading. For normal compressive loading, a strut-like architecture is found, with trabeculae oriented in the global load direction. The fact that no transversal struts were formed can be explained by the absence of transversal loads. The trabecular width in the generated models depends on the magnitude of the load, as demonstrated by the model with a ramp load applied. Under high loading, trabeculae tend to grow together, thus forming closed structures. Both the open and the closed structures are found in vertebral bodies or in the tibial plateau, where the main load is in uniaxial direction. The dense loaded surfaces found in these simulations then represent a subchondral bone layer.
For the combined compressive/shear loading a plate-like architecture was found. Such plate-like trabecular architectures are found for example in the acetabulum, where shear is the main loading type due to bending of the sandwich construction of the acetabulum. The dense end plates could then correspond to the thin cortical bone layer of the acetabulum [28].

Using the same model for the simulation of bone resorption after bone disuse, some typical resorption patterns were found. In all cases thinning of trabeculae was found, which is indeed a well-known phenomena in trabecular bone, related to aging and bone disuse [2,29,30]. In addition to the thinning of trabeculae, structural changes were found. For the model with uniaxial compressive loading, the closed void structure was changed to an open columnar structure, and for the compressive/shear loading model, the plates were perforated and transformed to trabeculae.

It was concluded that the present model provides a promising and well-performing method to explain many of the load-dependent characteristics of the trabecular architecture. Even for the relative simple (uniaxial) loading cases used in the present study, typical but non-trivial results are found. It is expected that more realistic three-dimensional load-cases can explain the function and adaptation of complex trabecular structures as seen in real bones.

Acknowledgements
This project was sponsored by The Netherlands Foundation for Research (NWO/Medical Sciences) and by the National Computing Facilities Foundation (NCF).

REFERENCES

1. Eriksen E.F. and Kassem M., The cellular basis of bone remodeling, Triangle 1992, Vol. 31, 45-57
2. Parfit A.M., The two-stage concept of bone loss revisited, Triangle 1992, Vol. 31, 99-110
3. Rodan G.A., Bourret L.A., Harvey A. and Mensi T., 3',5' Cyclic AMP and 3',5' cyclic GMP: mediators of the mechanical effects on bone remodeling, Science 1975, Vol. 189, 467-469
4. Frost H.M., Perspectives: bone's mechanical usage windows, Bone and Mineral 1992, Vol. 19, 257-271
5. Carter D.R., Fyhrie D.P. and Whalen R.T., Trabecular bone density and loading history: regulation of connective tissue biology by mechanical energy, J.Biomech. 1987, Vol. 20, 785-794
6. Beaupre G.S., Orr T.E. and Carter D.R., An approach for time-dependent bone modeling and remodeling -theoretical development, J.Orthop.Res. 1990, Vol. 8, 651-661
7. Huiskes R., Weinans H., Grootenboer H.J., Dalstra M., Fudala B. and Sloof T.J., Adaptive bone-remodeling theory applied to prosthethic-design analysis, J.Biomech. 1987, Vol. 20, 1135-1150
8. Weinans H., Huiskes R., Van Rietbergen B., Sumner D.R., Turner T.M. and Galante J.O., Adaptive bone remodeling around bonded noncemented total hip arthroplasty: a comparison between animal experiments and computer simulation, J.Orthop.Res. 1993, Vol. 11, 500-513
9. Van Rietbergen B., Huiskes R., Weinans H., Sumner D.R., Turner T.M. and Galante J.O., The mechanism of bone remodeling and resorption around press-fitted THA stems, J.Biomech. 1993, Vol. 26, 369-382
10. Beaupre G.S., Orr T.E. and Carter D.R., An approach for time-dependent bone modeling and remodeling -application: a preliminary remodeling simulation, J.Orthop.Res. 1990, Vol. 8, 662-670
11. Jacobs C.R. and Beaupre G.S., The role of multiple load histories in bone remodeling simulation, Trans. 38th Ann. Meeting ORS 1992, Vol. 535
12. Weinans H., Huiskes R. and Grootenboer H.J, The behavior of adaptive bone-remodeling simulation models, J.Biomech. 1992, Vol. 25, 1425-1441
13. Mullender M.G., Huiskes R. and Weinans H.,A physiological approach to the simulation of bone remodeling; in Transactions of the 39th Annual Meeting of the Orthopaedic Research Society. Chicago, IL, ORS, 1993, pp 531.
14. Mullender M.G., Huiskes R. and Weinans H., A physiological approach to the simulation of bone remodeling as a self organizational control process, J.Biomech. 1994 (in press)
15. Van Rietbergen B., Weinans H., Huiskes R., et al,Three dimensional analysis of a realistic trabecular bone structure, using a large-scale FE-model; in Langrana NA, Friedman MH, Grood ES (eds): BED Bioengineering Conference. New York, ASME, 1993, pp 250-253.
16. Van Rietbergen B., Weinans H., Huiskes R. and Odgaard A., A new method to determine trabecular bone elastic properties and loading using micro-mechanical Finite-Element models, J.Biomech. 1994 (in press)
17. Cowin S.C., Moss-Salentijn L. and Moss M.L., Candidates for the mechanosensory system in bone, J.Biomech.Eng. 1991, Vol. 113, 191-197
18. Jee W.S. and Frost H.M., Skeletal adaptations during growth, Triangle 1992,

Vol. 31, 77-88

19. Shih M.S., Cook M.A., Spence C.A., Palnitkar S., McElroy H. and Parfitt A.M., Relationship between bone formation rate and osteoblast surface on different subdivisions of the endosteal envelope in aging & osteoporosis, Bone 1993, Vol. 14, 519-521
20. Strang G., Introduction to applied mathematics. Wellesley, Massachusetts 02181, Wellesley-Cambridge Press, 1986.
21. Zienkiewicz O.C., The finite element method. Maidenhead, McGraw-Hill, 1977.
22. Hughes T.J.R., Levit I. and Winget J., An Element-By-Element solution algorithm for problems of structural and solid mechanics, Comp.Meth.in Appl.Mech.and Eng. 1983, Vol. 36, 241-254
23. Marotti G., Cane V., Palazzini S. and Palumbo C., Structure-function relationships in the osteocyte, Italian J.Min.&Elect.Metab. 1990, Vol. 4, 93-106
24. Rubin C.T., Skeletal strain and the functional significance of bone architecture, Calcif.Tissue Int. 1984, Vol. 36, S11-S18
25. Choi K., Kuhn J.L., Ciarelli M.J. and Goldstein S.A., The elastic moduli of human subchondral trabecular, and cortical bone tissue and the size dependency of cortical bone modulus, J.Biomech. 1990, Vol. 23, 1103-1113
26. Rho J.Y., Ashman R.B. and Turner C.H., Young's modulus of trabecular and cortical bone material: ultrasonic and microtensile measurements, J.Biomech. 1993, Vol. 26, 111-119
27. Currey J.D., The effect of porosity and mineral content on the Young's modulus of elasticity of compact bone, J.Biomech. 1988, Vol. 21, 131-139
28. Dalstra M., Huiskes R., Odgaard A. and Van Erning L., Mechanical and textural properties of pelvic trabecular bone, J.Biomech. 1993, Vol. 26, 523-535
29. Lips P., Courpron P. and Meunier P.J., Mean wall thickness of trabecular bone packets in the human iliac crest: Changes with age, Calcif. Tissues Res. 1978, Vol. 26, 13-17
30. Kragstrup J., Melsen J. and Mosekilde P.J., Thickness of bone formed at remodeling sites in normal human iliac trabecular bone: Variations with age and sex, Metab. Bone Dis. 1983, Vol. 5, 17-21